NANO LETTERS

2009
Vol. 9, No. 12
4359-4363

Transfer of Large-Area Graphene Films for High-Performance Transparent Conductive Electrodes

Xuesong Li,[†] Yanwu Zhu,[†] Weiwei Cai,[†] Mark Borysiak,[‡] Boyang Han,[†] David Chen,[†] Richard D. Piner,[†] Luigi Colombo,[*,§] and Rodney S. Ruoff[*,†]

Department of Mechanical Engineering and the Texas Materials Institute, The University of Texas at Austin, Austin, Texas 78712-0292, 2009 NNIN REU Intern at The University of Texas at Austin, Austin, Texas 78712-0292 and Texas Instruments Incorporated, Dallas, Texas 75243

Received August 11, 2009; Revised Manuscript Received September 18, 2009

ABSTRACT

Graphene, a two-dimensional monolayer of sp^2-bonded carbon atoms, has been attracting great interest due to its unique transport properties. One of the promising applications of graphene is as a transparent conductive electrode owing to its high optical transmittance and conductivity. In this paper, we report on an improved transfer process of large-area graphene grown on Cu foils by chemical vapor deposition. The transferred graphene films have high electrical conductivity and high optical transmittance that make them suitable for transparent conductive electrode applications. The improved transfer processes will also be of great value for the fabrication of electronic devices such as field effect transistor and bilayer pseudospin field effect transistor devices.

Graphene, a two-dimensional monolayer of sp^2-bonded carbon atoms, has been the focus of much research since its isolation because of the unique transport properties.[1,2] Because of graphene's high optical transmittance and conductivity it is also being considered as a transparent conductive electrode.[3−9] In comparison to traditional transparent conductive electrodes such as indium tin oxide (ITO), graphene films have high mechanical strength, are flexible, and are chemically stable.[5,6,9] Production of large-area and high-quality graphene films is necessary for electronic applications such as graphene field effect transistors (FETs),[10,11] newly introduced bilayer pseudospin field effect transistors (BiSFETs),[12] and transparent conductive electrodes.[3−9]

One method of making graphene is by nanomechanical cleavage of graphite but this method can only produce small area films of the order of a few tens of micrometers and is not scalable.[13] Chemical reduction of exfoliated graphite oxide layers can produce large quantities of reduced graphene oxide platelets that can be formed into thin films,[14] but the electrical properties do not rival those of exfoliated natural graphite. This is possibly due to a combination of factors, such as damage of the graphene lattice during the formation of graphite oxide into a colloidal suspension (particularly the use of ultrasonication to disperse the graphite oxide) or the creation of point defects during the reduction of graphite oxide.[15] Graphite has also been partially exfoliated and dispersed in certain solvents,[5,16] but the yield is still very low and the films made from such dispersions are not continuous. The discontinuity and nonuniform thickness of the aforementioned films yield high electrical resistance and low optical transmittance, which do not meet transparent electrode requirements.

Two other graphene synthesis approaches have been reported, graphitization of single crystal SiC[17,18] and growth on metal substrates.[9,19−23] Field effect transistors fabricated using synthetic graphene obtained on SiC and metal substrates have yielded devices with high mobility at room temperature demonstrating potential for electronic devices but the mobility is still not as high as graphene exfoliated from natural graphite. Graphene has been grown on a number of metals, among others Ru,[19] Ir,[20] Ni,[9,21,22] and more recently Cu.[23] Monolayer graphite (MG) or graphene (the MG nomenclature has been used by the surface science community since the 1970s) has been grown on many substrates.[24] However, most applications require that graphene to be on an insulator and this requires that if graphene is grown on a metal it must be transferred to another appropriate substrate or processed in some other way. Etching of Cu, Ni and Ru is relatively straightforward however wet etching

* To whom correspondence should be addressed. E-mail: (R.S.R.) r.ruoff@mail.utexas.edu; (L.C.) colombo@ti.com.
[†] Department of Mechanical Engineering and the Texas Materials Institute, The University of Texas at Austin.
[‡] 2009 NNIN REU Intern at The University of Texas at Austin.
[§] Texas Instruments Incorporated.

10.1021/nl902623y CCC: $40.75
Published on Web 10/21/2009

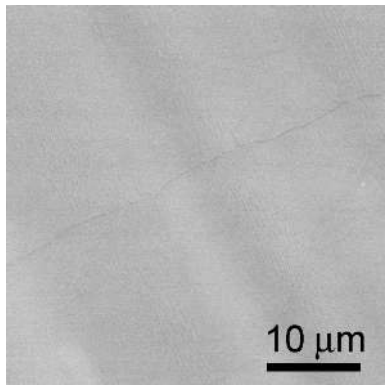

Figure 1. SEM image of as-grown graphene on Cu with a wrinkle.

of Ir is extremely difficult since it is one of its fundamental properties.[25] Further, the cost of Ru and Ir would be prohibitively high for implementation in large volume manufacturing in comparison to Ni and Cu.

We grew large-area graphene on Cu foils by taking advantage of the low C solubility in Cu[23] and used polymethyl-methacrylate (PMMA) to aid the transfer of graphene to other substrates.[9,22,23] This kind of transfer-printing method has also been used to transfer and align carbon nanotube arrays.[26] However, we found that the transfer process caused the graphene to form cracks upon transfer, due to the intrinsic mechanical properties on monolayer graphene and the method of transfer initially used. In this paper, we report an improved transfer process that yields a graphene film on SiO_2/Si with a much lower density of cracks or tears. The transferred graphene films show excellent optical transmission and electrical conductivity across a large area suggesting that the material could be a promising transparent conductive electrode.

The graphene films were grown on 25 μm thick Cu foils in a similar way to the previously reported process.[23] Figure 1 shows a scanning electron microscopy (SEM) image of a graphene film on a Cu foil after growth showing the presence of a wrinkle but no other significant macroscopic defects. A challenge is then on how to transfer this film onto another substrate without further degradation. The transfer flows of both the "old" and "new" methods are shown in Figure 2. Ideally, if the graphene films were perfectly flat, the old process would be efficient in transferring large-area graphene; however, because the surface of the metal goes through significant surface reconstruction at high temperatures the resulting metal surface tends to be rough and graphene tends to follow the surface of the underlying metal. When graphene is removed from the "rough" metal surface it does not lie flat on top of the target surface, for example, on a SiO_2/Si wafer, which in comparison is much smoother. As a result, there are always some small gaps between the graphene and the substrate surface, that is, the graphene does not make full contact with the SiO_2/Si substrate and the unattached regions tend to break easily and cracks are formed when the PMMA film is dissolved away (top-right inset in Figure 2). Part of the problem is that the PMMA is a hard coating after curing and when it is dissolved away, the graphene does not

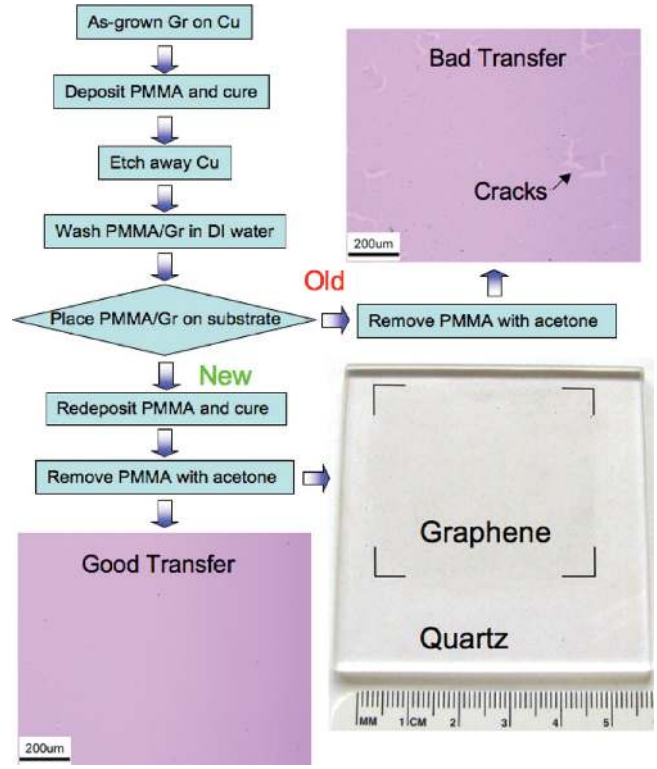

Figure 2. Processes for transfer of graphene films ("Gr" = graphene). The top-right and bottom-left insets are the optical micrographs of graphene transferred on SiO_2/Si wafers (285 nm thick SiO_2 layer) with "bad" and "good" transfer, respectively. The bottom-right is a photograph of a 4.5 × 4.5 cm^2 graphene on quartz substrate.

relax. We found that the graphene transfer process was improved by introducing a second PMMA coating step after the PMMA/graphene was placed on the SiO_2/Si substrate. After placing the PMMA/graphene stack on the target substrate, an appropriate amount of liquid PMMA solution was dropped on the cured PMMA layer thus partially or fully dissolving the precoated PMMA. The redissolution of the PMMA tends to mechanically relax the underlying graphene, leading to a better contact with the substrate. The bottom-left inset in Figure 2 shows an optical micrograph of a graphene film transferred onto a SiO_2/Si wafer showing excellent continuity over a millimeter length scale with very few cracks, and the bottom-right inset is a photo of a graphene film with a size of 4.5 × 4.5 cm^2 on a quartz substrate. We believe that this improved method provides a pathway to significantly improve large-area graphene transfer.

The growth uniformity and transfer efficiency were further evaluated by optical microscopy and micro Raman spectroscopy. Figure 3a shows an optical micrograph of a 50 × 50 μm^2 graphene film. The uniform color contrast of the optical micrograph indicates that the film has excellent thickness uniformity[27] but it also shows the presence of dark lines that are associated with wrinkles which are believed to form during cool-down as a result of the difference in coefficient of thermal expansion between the graphene and the Cu substrate.[28] The inset in Figure 3a shows a Raman spectrum (WITec alpha300 with a laser wavelength of 532 nm, × 100 objective lens) with peaks typical for graphene,

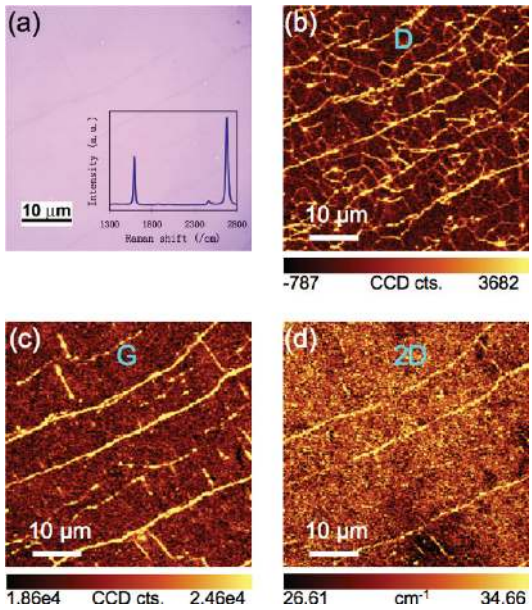

Figure 3. Optical microscopy and micro-Raman spectroscopy images. (a) Optical image of graphene on SiO_2/Si wafer. Inset in (a) is a Raman spectrum from this film showing the basic features of graphene. (b−d) Raman maps of integrated intensity of the D (1300−1400 cm^{-1}) and G (1560−1630 cm^{-1}) bands, and fwhm of 2D (2620−2740 cm^{-1}) bands, respectively, corresponding to the area in (a).

including a 2D-band with a full width half-maximum (fwhm) of ∼28 cm^{-1} located at ∼2680 cm^{-1}.[22,29] In addition, the intensity of the D-band at ∼1350 cm^{-1}, a measure of defects in the graphene, is below the Raman detection limit. This is further demonstrated by a low D-band intensity map (Figure 3b) across most of the film except at wrinkled regions. It should be noted that the D-band map is more sensitive to wrinkles than the optical micrograph, and the G- and 2D-band maps. The G- and 2D-band maps (Figure 3c,d) show that the film is graphene and that it is continuous.

Because of its high conductivity and optical transmittance, graphene can be used as a transparent conductive electrode. Figure 4 shows the sheet resistance of graphene/PMMA (measured by the van der Pauw method) as it is bent multiple times for different radii of curvature, r. The graphene/PMMA was placed on a 0.3 mm thick polyethylene terepthalate (PET) substrate. The PMMA film is only hundreds of nanometers thick and the PET thickness alone is used in the tensile strain calculation. The sheet resistance is calculated using the formula: $R_s = (\pi/\ln 2)[(R_x + R_y)/2]f$, where f is a factor that is a function only of the ratio of R_y/R_x.[30] For a flat graphene layer on PMMA, the sheet resistance, R_s, is ∼350 Ω/□. When the film was bent, R_x is independent of the bending radius while R_y is nearly invariant for $r = 3$ mm (approximate tensile strain of 5%) even after 100 bending cycles. But when r was decreased to about 1 mm (approximate tensile strain of 15%), R_y increased by about a factor of 2. The increase in R_y may be attributed to excess stretching of graphene but even for this case, the sheet resistance is still low, <500 Ω/□. The bending test results suggest that our graphene films have excellent mechanical stability, and while slightly lower than that of the few-layer

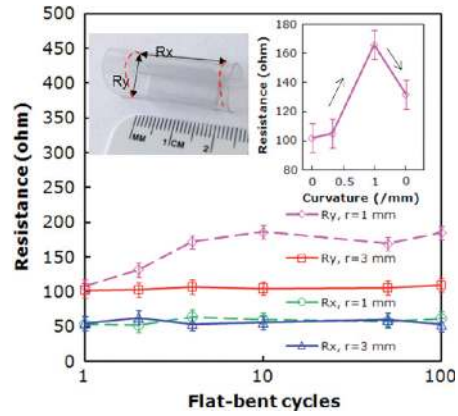

Figure 4. Resistance of graphene/PMMA films with different bending radii and flat-fold cycles. The top left inset shows the photo of bent graphene/PMMA/PET. The red dashed lines mark the edges of graphene/PMMA film. The top right inset shows the changes of R_y as a function of bending radius.

graphene films grown on Ni substrates,[9] they are superior to conventional materials used in flexible electronics.[31]

Figure 5 shows a summary of the electrical and optical properties of graphene synthesized on Cu. The transmittance of our graphene films was measured by placing the graphene on a cover glass as a single layer and as multiple stacked layers. Multiple layer "graphene stacks" were created using the transfer process sequentially, and the resulting films are shown in Figure 5a. The transmittance of the films was measured using a spectroscopic ellipsometer (JA Woolam, M-2000) where a bare cover glass was used as a reference. The transmittance data as a function of wavelength for the four films are shown in Figure 5b with the inset showing the transmittance at $\lambda = 550$ nm as a function of the number of stacked graphene layers in each of the films. By fitting the data to Beer's law, an attenuation coefficient $\alpha = 2.6\%$ per layer is extracted which is very close to the theoretical value of 2.3%.[4,5] The higher attenuation for our films is perhaps due to the existence of wrinkles.

Figure 5c shows the sheet resistances of graphene films transferred on cover glass measured by the van der Pauw method. The sheet resistance of graphene is 2.1 kΩ/□ whereas that of four layers of graphene is 350 Ω/□ while still maintaining a relatively high transmittance of about 90%. Theoretically, the sheet resistance of a graphene film, R_{s1}, should be constant and related to that of a multilayer film, R_{sn}, if all layers are acting independently of each other, as $R_{sn} = R_{s1}/n$, where n is the number of graphene layers. However, Figure 5c shows that the average sheet resistance of our films decreases slightly by stacking the films. The discrepancy might be explained by considering that the cracks in one film are bridged by its neighboring films thus increasing the conductivity. We also find that the sheet resistance of graphene films transferred onto a glass substrate is higher than that of graphene/PMMA films. The difference may be attributed to a couple of factors (1) the graphene films transferred on glass substrates have more cracks and (2) PMMA may be affecting the sheet resistance of the graphene film.[32]

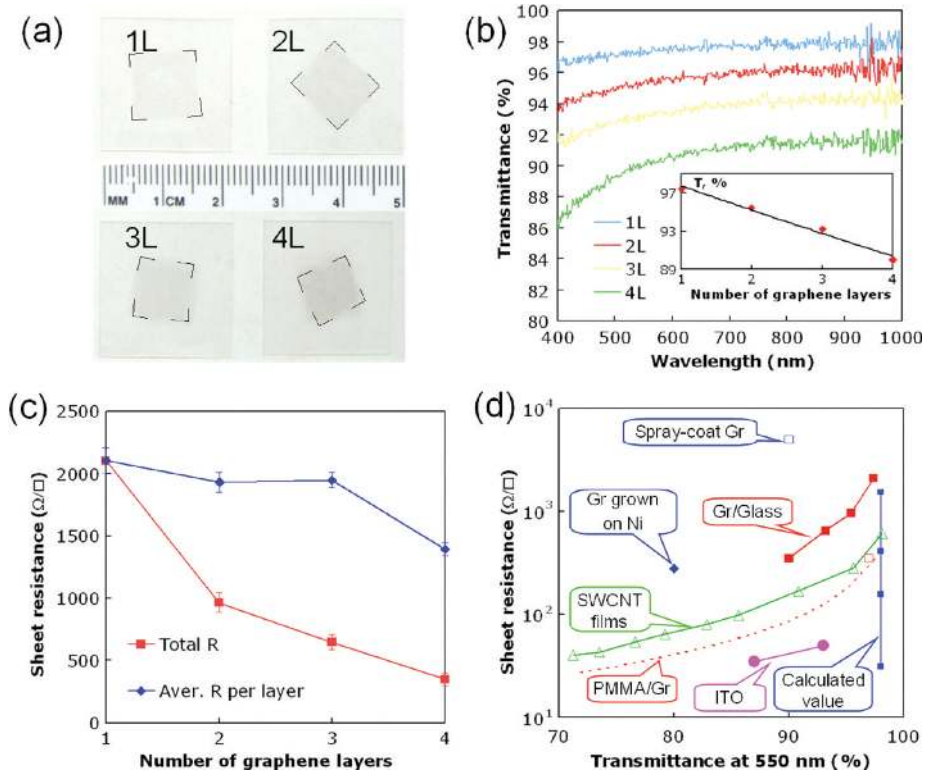

Figure 5. Evaluation of graphene films as transparent conductive electrodes. (a) Photographs of 1 cm^2 films with 1 up to 4 layers of stacked graphene films on cover glass slips. (b) Transmittance of *n*-layer graphene films shown in (a). The inset is the relationship between the transmittance, *T* (%), at $\lambda = 550$ nm as a function of the number of stacked graphene layers, *n*. (c) Sheet resistance of *n*-layer graphene films as a function of the number of stacked graphene layers, *n*. (d) Comparison of transparent conductive films, legend: red closed square and red open square, this work graphene on glass and PMMA, respectively, the dashed line is an extension for more stacked graphene layers calculated based on the derived attenuation coefficient and the sheet resistance of graphene on PMMA; blue open square,[5] spray-coated graphene film; blue diamond,[9] graphene grown on Ni and transferred onto polydimethylsiloxane substrate; green open triangle,[33] SWCNT films; pink closed circle,[34,35] ITO; blue closed square, calculated sheet resistance of graphene with a carrier density of 10^{12} cm^{-2} based on four different mobilities, 4050 cm V^{-1} s^{-1} for CVD grown graphene,[23] 15 000 cm V^{-1} s^{-1} for exfoliated graphene,[1] 40 000 cm V^{-1} s^{-1} of the extrinsic limit (scattering by the surface of the substrate, e.g., SiO_2) and 200 000 cm V^{-1} s^{-1} of the intrinsic limit (scattering by the acoustic phonons of graphene).[38]

Figure 5d shows the comparison of the sheet resistance of our graphene films with other sources of graphene, single-walled carbon nanotube (SWCNT) films, and ITO, as a function of transmittance at $\lambda = 550$ nm. At this time the graphene films formed by spray-coating exfoliated graphite dispersions have the highest sheet resistance.[5] In comparison to graphene grown on Ni,[9] the graphene grown on Cu and transferred onto glass substrate has higher transmittance with comparable sheet resistance while that on PMMA has even lower sheet resistance than SWCNT films.[33] However the sheet resistance of graphene films is still not as low as that of ITO,[34,35] but the current results fulfill the requirements for some applications such as electrostatic dissipation, cathode ray tubes, touch screens, and flat panel displays.[36] The use of graphene for transparent conductive electrode applications such as for photovoltaic applications still remains a challenge since the desired sheet resistance is as low as a few tens of ohms/sq or even lower.[37] Chen et al. report that the intrinsic sheet resistance of graphene is about 30 Ω/□,[38] indicating that there is still potential for improving quality of graphene for use in transparent conductive electrode applications.

In summary, we have synthesized large area graphene and improved its transfer to other substrates. The low sheet resistance and high transmittance make it an attractive candidate for some transparent electrode applications. The synthesis and transfer techniques can be scaled, and it appears as if there are no limitations on the size of the graphene films except for the dimensions of the substrate and growth system. The improved transfer processes will also useful for the fabrication of electronic devices such as FETs and BiSFET devices.

Methods. ***Transfer of Graphene Films.*** (1) As-grown graphene film on Cu foil was drop-coated with PMMA (average M_w ~996 000 by GPC, Sigma-Aldrich product no. 182265, dissolved in chlorobenzene with a concentration of 46 mg/mL), which was then cured at 180 °C for 1 min. (2) Since graphene grows on both sides of the Cu foil after one side of the Cu/graphene was coated with PMMA the opposite side was polished to remove the graphene layer. The 1 × 1 cm^2 × 25 μm thick Cu substrate was then etched away by an aqueous solution of iron nitrate (0.05 g/mL) over a period of ~12 h. The PMMA/graphene stack was washed with deionized water and placed on the target substrates and dried. (4) After the transfer to the targeted substrate a small amount of liquid PMMA solution was dropped onto the PMMA/graphene to dissolve the precoated PMMA. (5) The new

PMMA film was then slowly cured at room temperature for about 30 min and then dissolved by acetone.

Acknowledgment. X.L. and R.S.R. would like to thank The University of Texas at Austin for support. L.C. appreciates support from the Nanoelectronic Research Initiative (NRI-SWAN; no. 2006-NE-1464).

References

(1) Geim, A. K.; Novoselov, K. S. *Nat. Mater.* **2007**, *6*, 183–191.
(2) Geim, A. K. *Science* **2009**, *324* (19), 1530–1534.
(3) Watcharotone, S.; Dikin, D. A.; Stankovich, S.; Piner, R.; Jung, I.; Dommett, G. H. B.; Evmenenko, G.; Wu, S. E.; Chen, S. F.; Liu, C. P.; Nguyen, S. T.; Ruoff, R. S. *Nano Lett.* **2007**, *7* (7), 1888–1892.
(4) Nair, R. R.; Blake, P.; Grigorenko, A. N.; Novoselov, K. S.; Booth, T. J.; Stauber, T.; Peres, N. M. R.; Geim, A. K. *Science* **2008**, *320*, 1308.
(5) Blake, P.; Brimicombe, P. D.; Nair, R. R.; Booth, T. J.; Jiang, D.; Schedin, F.; Ponomarenko, L. A.; Morozov, S. V.; Gleeson, H. F.; Hill, E. W.; Geim, A. K.; Novoselov, K. S. *Nano Lett.* **2008**, *8* (6), 1704–1708.
(6) Wang, X.; Zhi, L.; Müllen, K. *Nano Lett.* **2008**, *8* (1), 323–327.
(7) Li, X.; Zhang, G.; Bai, X.; Sun, X.; Wang, X.; Wang, E.; Dai, H. *Nat. Nanotechnol.* **2008**, *3*, 538–542.
(8) Becerril, H. A.; Mao, J.; Liu, Z.; Stoltenberg, R. M.; Bao, Z.; Chen, Y. *ACS Nano* **2008**, *2* (3), 463–470.
(9) Kim, K. S.; Zhao, Y.; Jang, H.; Lee, S. Y.; Kim, J. M.; Kim, K. S.; Ahn, J.-H.; Kim, P.; Choi, J.-Y.; Hong, B. H. *Nature* **2009**, *457*, 706–710.
(10) Kim, S.; Nah, J.; Jo, I.; Shahrjerdi, D.; Colombo, L.; Yao, Z.; Tutuc, E.; Banerjee, S. K. *Appl. Phys. Lett.* **2009**, *94*, 062107.
(11) Lemme, M. C.; Echtermeyer, T. J.; Baus, M.; Szafranek, B. N.; Bolten, J.; Schmidt, M.; Wahlbrink, T.; Kurz, H. *Solid-State Electron.* **2008**, *52* (4), 514–518.
(12) Banerjee, S. K.; Register, L. F.; Tutuc, E.; Reddy, D.; MacDonald, A. H. *IEEE Electron Device Lett.* **2009**, *30* (2), 158–160.
(13) Novoselov, K. S.; Geim, A. K.; Morozov, S. V.; Jiang, D.; Zhang, Y.; Dubonos, S. V.; Grigorieva, I. V.; Firsov, A. A. *Science* **2004**, *306*, 666–669.
(14) Park, S.; Ruoff, R. S. *Nat. Nanotechnol.* **2009**, *4*, 217–224.
(15) Paredes, J. I.; Villar-Rodil, S.; Solís-Fernández, P.; Martínez-Alonso, A.; Tascón, J. M. D. *Langmuir* **2009**, *25* (10), 5957–5968.
(16) Hernandez, Y.; Nicolosi, V.; Lotya, M.; Blighe, F. M.; Sun, Z.; De, S.; McGovern, I. T.; Holland, B.; Byrne, M.; Gun'Ko, Y. K.; Boland, J. J.; Niraj, P.; Duesberg, G.; Krishnamurthy, S.; Goodhue, R.; Hutchison, J.; Scardaci, V.; Ferrari, A. C.; Coleman, J. N. *Nat. Nanotechnol.* **2008**, *3*, 563−568.
(17) Berger, C.; Song, Z.; Li, X.; Wu, X.; Brown, N.; Naud, C.; Mayou, D.; Li, T.; Hass, J.; Marchenkov, a. A. N.; Conrad, E. H.; First, P. N.; de Heer, W. A. *Science* **2006**, *312*, 1991–1996.
(18) Emtsev, K. V.; Bostwick, A.; Horn, K.; Jobst, J.; Kellogg, G. L.; Ley, L.; McChesney, J. L.; Ohta, T.; Reshanov, S. A.; Rohrl, J.; Rotenberg, E.; Schmid, A. K.; Waldmann, D.; Weber, H. B.; Seyller, T. *Nat. Mater.* **2009**, *8* (3), 203–207.
(19) Sutter, P. W.; Flege, J.-I.; Sutter, E. A. *Nat. Mater.* **2008**, *7*, 406–411.
(20) Coraux, J.; N'Diaye, A. T.; Busse, C.; Michely, T. *Nano Lett.* **2008**, *8* (2), 565–570.
(21) Yu, Q.; Lian, J.; Siriponglert, S.; Li, H.; Chen, Y. P.; Pei, S.-S. *Appl. Phys. Lett.* **2008**, *93*, 113103.
(22) Reina, A.; Jia, X.; Ho, J.; Nezich, D.; Son, H.; Bulovic, V.; Dresselhaus, M. S.; Kong, J. *Nano Lett.* **2009**, *9*, 30–35.
(23) Li, X. S.; Cai, W. W.; An, J. H.; Kim, S.; Nah, J.; Yang, D. X.; Piner, R. D.; Velamakanni, A.; Jung, I.; Tutuc, E.; Banerjee, S. K.; Colombo, L.; Ruoff, R. S. *Science* **2009**, *324*, 1312–1314.
(24) Greber, T. Graphene and Boron Nitride Single Layers. *Cond-Mat.Mtrl-Sci* [Online], April 9, 2009, arXiv:0904.1520v1. arXiv.org. Accessed October 15, 2009.
(25) http://www.webelements.com/iridium/. Accessed October 15, 2009.
(26) Kang, S. J.; Kocabas, C.; Kim, H. S.; Cao, Q.; Meitl, M. A.; Khang, D. Y.; Rogers, J. A. *Nano Lett.* **2007**, *7* (11), 3343–3348.
(27) Ni, Z. H.; Wang, H. M.; Kasim, J.; Fan, H. M.; Yu, T.; Wu, Y. H.; Feng, Y. P.; Shen, Z. X. *Nano Lett.* **2007**, *7* (9), 2758–2763.
(28) Obraztsov, A. N.; Obraztsova, E. A.; Tyurnina, A. V.; Zolotukhin, A. A. *Carbon* **2007**, *45*, 2017–2021.
(29) Ferrari, A. C.; Meyer, J. C.; Scardaci, V.; Casiraghi, C.; Lazzeri, M.; Mauri, F.; Piscanec, S.; Jiang, D.; Novoselov, K. S.; Roth, S.; Geim, A. K. *Phys. Rev. Lett.* **2006**, *97*, 187401.
(30) Van der Pauw, L. J. *Philips Tech. Rev.* **1958**, *20*, 220–224.
(31) Lewis, J. *Mater. Today* **2006**, *9*, 38–45.
(32) Lohmann, T.; von Klitzing, K.; Smet, J. H. *Nano Lett.* **2009**, *9*, 1973–1979.
(33) Geng, H.-Z.; Kim, K. K.; So, K. P.; Lee, Y. S.; Chang, Y.; Lee, Y. H. *J. Am. Chem. Soc.* **2007**, *129*, 7758–7759.
(34) Kim, H.; Horwitz, J. S.; Kushto, G. P.; Kafafi, Z. H.; Chrisey, D. B. *Appl. Phys. Lett.* **2001**, *79*, 284–286.
(35) Wong, F. L.; Fung, M. K.; Tong, S. W.; Lee, C. S.; Lee, S. T. *Thin Solid Films* **2004**, *466*, 225–230.
(36) Kaempgen, M.; Duesberg, G. S.; Roth, S. *Appl. Surf. Sci.* **2005**, *252*, 425–429.
(37) Granqvist, C. G. *Sol. Energy Mater. Sol. Cells* **2007**, *91*, 1529–1598.
(38) Chen, J. H.; Jang, C.; Xiao, S.; Ishigami, M.; Fuhrer, M. S. *Nat. Nanotechnol.* **2008**, *3*, 206–209.

NL902623Y